Chinese Chemical Letters 36 (2025) 110465

Contents lists available at ScienceDirect

Chinese Chemical Letters

journal homepage: www.elsevier.com/locate/cclet

Multiple host-guest and metal coordination interactions induce supramolecular assembly and structural transition

Shengyong Liu[a], Hui Li[a,*], Wei Zhang[a], Yan Zhang[a], Yan Dong[a], Wei Tian[b,*]

[a] Jiangxi Province Key Laboratory of Functional Crystalline Materials Chemistry, School of Chemistry and Chemical Engineering, Jiangxi University of Science and Technology, Ganzhou 341000, China
[b] Shaanxi Key Laboratory of Macromolecular Science and Technology, School of Chemistry and Chemical Engineering, Northwestern Polytechnical University, Xi'an 710072, China

ARTICLE INFO

Article history:
Received 28 June 2024
Revised 1 September 2024
Accepted 13 September 2024
Available online 15 September 2024

Keywords:
Self-assembly
Supramolecular chemistry
Macrocycles
Host-guest interaction
Metal coordination

ABSTRACT

Three monomers, namely A2, B2, and GH, were designed and synthesized. By utilizing double host-guest interactions, the monomers A2+B2+GH underwent self-assembly to form a supramolecular linear polymer (SLP) at high concentrations. Long fibers could be pulled from the concentrated SLP solution. Upon the addition of $PdCl_2(PhCN)_2$ into the SLP solution, a structural transformation occurred from SLP to a supramolecular crosslinked polymer (SCP) through metal coordination interaction. This transformation induced fluorescence quenching, test paper strips for ion detection experiment confirmed that the SLP had good detection ability for Pd^{2+}. Furthermore, the SCP underwent a transformation into a gel when the concentration exceeded 145 mmol/L. The SCP gel demonstrated sensitivity to different stimuli, such as K^+ ions and changes in temperature, accompanied by a reversible transition between sol and gel states. Additionally, rheological analyses indicated that the gel possessed favorable self-healing properties.

The phenomenon of supramolecular self-assembly involves the spontaneous formation of well-organized structures [1,2]. where structural units such as molecules, molecular groups, nanoscale aggregates, and nanomaterials come together to form stable aggregates with specific structures and functions through self-assembly [3-10]. For example, it is believed that the double helix structure of DNA and protein folding are outcomes of supramolecular self-assembly [11]. The process of supramolecular self-assembly primarily relies on non-covalent interactions, which include hydrogen bonding [12-14], host-guest interaction [15-18], charge transfer [19], metal coordination [20-22], π-π packing interaction [23], *etc*. Unlike covalent interactions, the dynamic reversibility of noncovalent interactions gives prepared functional materials unique properties such as stimuli-responsiveness, morphological variability, self-healing ability, and degradability [24-32]. These characteristics provide supramolecular assemblies with a wide array of application, including the delivery and release of drugs [33,34], catalytic reactions [35], and the conversion of energy [36,37]. Supramolecular self-assembly has emerged as a prominent strategy for the bottom-up construction of diverse functional materials.

Host-guest interactions, as one type of noncovalent interactions, have been widely applied to construct various supramolecular species [38]. Owing to their distinctive chemical and physical characteristics, macrocyclic host molecules such as crown ethers and pillararenes have been extensively applied in the synthesis of diverse supramolecular species [39-44]. On the other hand, metal-ligand coordination, as another significant type of noncovalent interaction, offers excellent directivity and strong binding capability [45-48]. These attributes facilitate different coordination geometries and endow the supramolecular coordination species with ample stability. Additionally, by incorporating functional groups into monomers beforehand, various functional supramolecular assemblies can be created by virtue of the self-assembly of monomers. Over recent decades, numerous supramolecular assemblies have been created utilizing metal coordination or host-guest interactions, some of which have practical applications in the fields of photoelectricity, biomedicine, and photocatalysis [33-37]. Although supramolecular assemblies can be easily prepared by various noncovalent interactions, little effort has been made to study the continuous preparation of supramolecular assemblies by using multiple host-guest interactions and metal coordination combined with fluorescent dyes. Thus, it is desirable to develop new supramolecular polymers with novel structures by utilizing multiple noncovalent interactions and to study their intriguing functionalities.

* Corresponding authors.
E-mail addresses: lh@jxust.edu.cn (H. Li), happytw_3000@nwpu.edu.cn (W. Tian).

https://doi.org/10.1016/j.cclet.2024.110465
1001-8417/

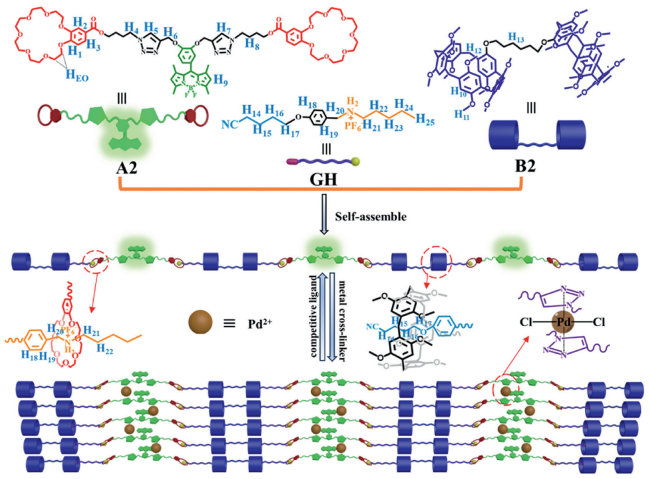

Scheme 1. Chemical structures of monomers A2, B2, GH, and a schematic illustration of the formation of the supramolecular polymers.

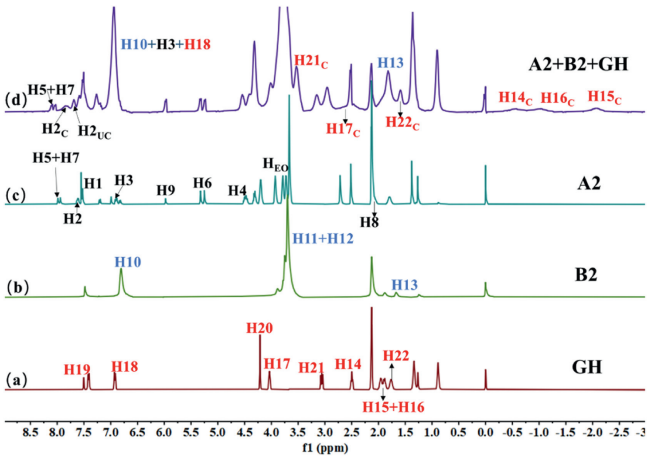

Fig. 1. ^{1}H NMR (400 MHz, chloroform-d_3/acetone-d_3 = 3:1, 293 K) spectra of (a) GH, (b) B2, (c) A2, (d) an equimolar mixture of A2+B2+GH (A2 = 25 mmol/L). The peaks corresponding to the complexed monomers were designated as c.

Boron-dipyrromethene (BODIPY) and its derivatives, known as porphyrin analogs, are important fluorescent dyes [49,50]. BODIPY has a high emission quantum yield, tunable photophysical properties, and excellent chemical durability. In this study, we incorporated a BODIPY fluorescent dye group into a monomer and fashioned two supramolecular polymers utilizing double host-guest interactions and metal coordination. Specifically, we designed three monomers: the homoditopic monomer A2, featuring two crown ethers (B21C7) and a boron-dipyrromethene core; the homoditopic monomer B2, comprising two pillararene (P5) groups; and the monomer GH, consisting of an ammonium salt (DA) moiety and a neutral alkyl (TPN) moiety. The combination of A2, B2, and GH can self-assemble into a linear supramolecular polymer SLP by double host-guest recognitions, which can further transform into a supramolecular crosslinked polymer SCP by metal coordination (Scheme 1).

To explore the self-organization of monomers A2+B2+GH in a blended solvent, we initially prepared four model compounds **1**–**4** (Fig. S1 in Supporting information). The ^{1}H NMR spectra of various mixtures containing model compounds were analyzed in a solvent of $CDCl_3$–CD_3COCD_3 (in a ratio of 3:1, v/v). When equimolar amounts of compounds **1** and **3** were combined in the solution, the complexity of the resulting ^{1}H NMR spectrum increased compared to that of individual model compounds (Fig. S2 in Supporting information), indicating a slow exchanging reaction between B21C7 and DA [51]. When combining compounds **2** and **4** in solvent, noticeable changes in chemical shifts were observed for protons H_{14-17} on compound **4** (Fig. S3 in Supporting information), signifying binding interaction involving P5-TPN in solution [52]. The analysis of the ^{1}H NMR spectra also indicated that B21C7 was unable to bind TPN while P5 could not bind DA when using a polar mixed solvent of $CDCl_3$–CD_3COCD_3 (Figs. S4 and S5 in Supporting information). Furthermore, when mixing compounds **1** + **2** + **3** + **4** together in the solvent (Fig. S6 in Supporting information), the ^{1}H NMR clearly revealed that the binding between **1** and **2** and the complexation between **3** and **4** was orthometric.

After confirming the self-sorting binding of the model compounds, we studied the self-assembly behaviour of the monomers in solution. The presence of double noncovalent interactions P5-TPN and B21C7-DA in A2+B2+GH resulted in the observation of a complex ^{1}H NMR spectrum (Fig. 1d). The chemical shifts of the protons were accurately determined by comparing the ^{1}H NMR spectra of model compounds and analyzing the ^{1}H–^{1}H COSY NMR spectrum of A2+B2+GH (Fig S7 in Supporting information). As depicted in Fig. 1d, H_{14}–H_{17} on monomer GH exhibited noticeable upfield shifts, confirming the binding between P5-TPN [50].

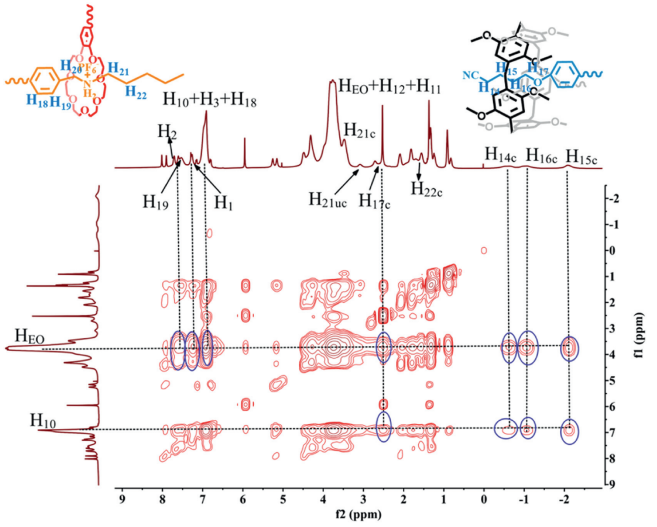

Fig. 2. 2D NOESY NMR (400 MHz, 293 K, 100 mmol/L) spectrum of A2+B2+GH in $CDCl_3$–CD_3COCD_3.

Protons H_2 on A2 and H_{21} on GH experienced downfield shifts, supporting the complexation of B21C7-DA [49]. Additionally, correlations between H_{18-19} on GH and H_{EO} on A2, as well as between H_{10-12} on B2 and H_{14-17} on GH were also observed in the 2D NOESY spectrum (Fig. 2), further substantiating the self-sorting binding between B21C7-DA and P5-TPN. The ^{1}H NMR spectra of A2+B2+GH gradually broadened with increasing monomer concentrations (Fig. S10 in Supporting information), indicating that a linear supramolecular polymer SLP with higher molecular weight was formed.

Considering that 1,2,3-triazole can form coordinated structure with metal ions, it was expected that adding palladium ion would transform this linear SLP into a supramolecular crosslinked polymer SCP. Gradual addition of $PdCl_2(PhCN)_2$ to the SLP solution resulted in downfield shifting of protons H_5 and H_7 on the 1,2,3-triazole moiety and broadening resonance peaks (Fig. S11 in Supporting information). This phenomenon indicated the complexation between triazole ligands and palladium(II) ion leading to the formation of a supramolecular crosslinked polymer network SCP when $PdCl_2(PhCN)_2$ was introduced into the SLP solution.

The formation of SLP and SCP was further investigated using 2D DOSY NMR (diffusion ordered spectroscopy). By altering the

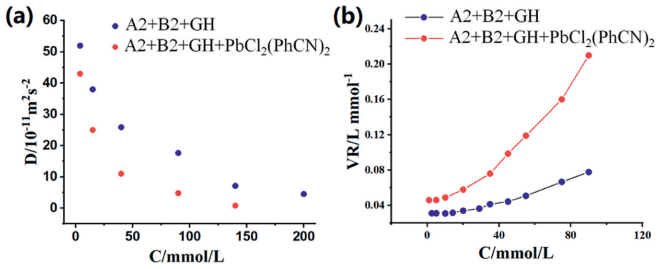

Fig. 3. (a) The diffusion coefficient values of A2+B2+GH and A2+B2+GH+$PbCl_2(PhCN)_2$ against the concentration of A2 (500 MHz, 293 K, A2:B2:GH:Pd^{2+} = 1:1:1:1). (b) Reduced viscosity (V_R) of SLP and SCP as a function of monomer concentration.

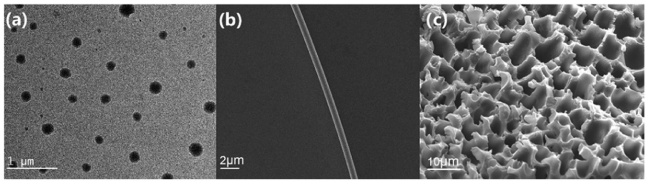

Fig. 4. (a) The representative TEM image of A2+B2+GH (25 mmol/L). (b) SEM image of a fiber pulled from a concentrated solution of A2+B2+GH (220 mmol/L). (c) SEM image of SCP xerogel.

monomer concentrations within the range of 4–200 mmol/L, a noticeable decline in the diffusion coefficient (D) of the A2+B2+GH system was observed, ranging from 5.19×10^{-10} m^2/s to 4.51×10^{-11} m^2/s (Fig. 3a). This result suggested that supramolecular polymerization was influenced by changes in concentration. The more than tenfold decrease in D data provides significant evidence supporting the formation of a supramolecular polymer [20]. The experimental value ($D_{200/4} = 11$) supported the formation of SLP. After further adding equimolar $PdCl_2(PhCN)_2$ to the A2+B2+GH solution (A2 = 140 mmol/L), the diffusion coefficient (D) decreased from 7.15×10^{-11} m^2/s to 8.42×10^{-12} m^2/s (Fig. 3a), indicating that a higher molecular weight crosslinked SCP was formed after the addition of $PdCl_2(PhCN)_2$.

Viscosity experiment was also performed to investigate the formation of SLP and SCP. The viscosities of A2+B2+GH and A2+B2+GH+$PdCl_2(PhCN)_2$ were measured at different concentrations, and corresponding plots were generated. Notably, the specific viscosity of A2+B2+GH showed a change in slope around 28 mmol/L (Fig. S14 in Supporting information). Initially, the curve had a slope of 1.03 at low concentrations. However, upon surpassing 28 mmol/L, the slope of curve changed into 1.74, indicating a transformation from low molecular weight oligomers to larger supramolecular polymers [53]. Furthermore, the reduced viscosity of A2+B2+GH+$PdCl_2(PhCN)_2$ displayed a significant exponential increase as monomer concentration rose (Fig. 3b), suggesting the growth in crosslinked SCP network with increasing sizes.

The morphologies of supramolecular polymers SLP and SCP were subsequently examined. A representative TEM image, obtained from the solution of A2+B2+GH, revealed the presence of spherical nanostructures (Fig. 4a). It should be noted that the TEM is difficult to observe the real chain structure of supramolecular polymer at the molecular level due to the limitations of the microtechnique. When the SLP was transformed from the solution to the dry state, which may induce the secondary assembly of SLP due to the dynamics of noncovalent bonds [54]. Since both monomers A2 and B2 contain flexible alkyl chain, the globular morphology may result from the entanglement and twisting of linear SLP, similar spherical morphologies of supramolecular linear polymers have also been observed in some reported literature [52,53]. SEM experiment provided further evidence for

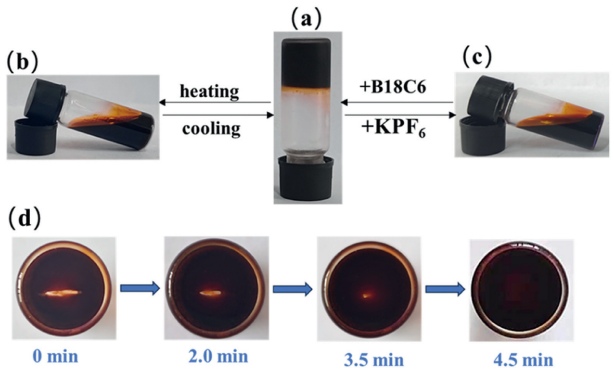

Fig. 5. (a) Photograph of the supramolecular gel. (b, c) Sol-gel transition at different conditions. (d) Self-repairing photograph of supramolecular gel.

the formation of SLP. A highly concentrated sample of A2+B2+GH (220 mmol/L) was prepared and rod-like fibers could be easily pulled from this concentrated solution using a pin (Fig. 4b). The SEM analysis demonstrated that the diameter of the fiber was approximately 1 μm, the anisotropic structures (1D fibers) resulted from the stretching of the entangled supramolecular linear polymer chains when an external force was applied to the viscous solution of concentrated SLP. After $PdCl_2(PhCN)_2$ was introduced into the solution of SLP, the SLP underwent a transformation to form the SCP through metal coordination. The network morphology of the SCP was revealed in the representative TEM image (Fig. S15b in Supporting information). As a gel was formed when the concentration of SCP was more than 145 mmol/L (Fig. 5a). To observe the actual morphology of the SCP gel, a gel sample was prepared at a concentration of 180 mmol/L. The gel was then immediately cooled in liquid nitrogen and subjected to freeze-drying. The morphology of the obtained xerogel was then examined by SEM, and the SEM image revealed the 3D network morphology of the xerogel prepared by the freeze-drying method (Fig. 4c).

The stimuli-responsiveness of supramolecular polymers were then examined. We conducted a study on the effects of adding or removing K^+ ions, considering their ability to bind with B21C7 [51]. The addition of KPF_6 to the solutions of SLP resulted in simplified ^1H NMR spectrum (Fig. S16 in Supporting information), indicating that the interaction of B21C7-DA on the skeletons of SLP was disrupted owing to the stronger complexation between B21C7 and potassium ion, leading to disassembly of SLP [51]. Furthermore, when we introduced a smaller crown ether, B18C6, into the solution, we observed the binding of B21C7-DA again, confirming the restructuring of SLP. Similarly, by introducing a competitive guest molecule (Fig. S17 in Supporting information), the complexation between P5-TPN could also be regulated. In the case of SLP, upon the addition of butanedinitrile to its solution, changes in the ^1H NMR spectrum revealed that the binding of butanedinitrile-P5 replaced the complexation of P5-TPN. This was evidenced by the disappearance of complexed protons H_{14}–H_{17} and the appearance of new complexed protons Ha (−1.33 ppm). These findings signified that SLP underwent a disassembly process after adding butanedinitrile. Since a gel was formed when the concentration of SCP exceeded 145 mmol/L (Fig. 5a), the responsiveness of the gel to external stimuli was subsequently investigated. When the gel was heated, it underwent a transition to form a sol, which could reversibly transform back into a gel upon cooling due to the presence of reversible noncovalent interactions (Fig. 5b). Furthermore, the addition of KPF_6 to the gel also leaded to its transformation into a sol as a result of B21C7-DA complexation collapse on the SCP backbone (Fig. 5c). When B18C6 was subsequently introduced to the sol, the recovery of B21C7-DA complexation enabled the reformation of a gel.

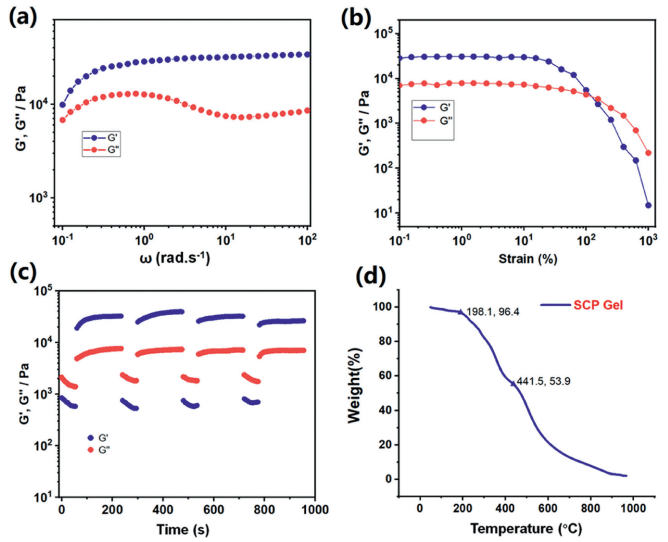

Fig. 6. (a) Gel subjected to a frequency sweep test. (b) Strain test of the gel. (c) Step strain experiments conducted by alternating strains between 300% and 0.1%. (d) Thermogravimetric analysis curve of the gel.

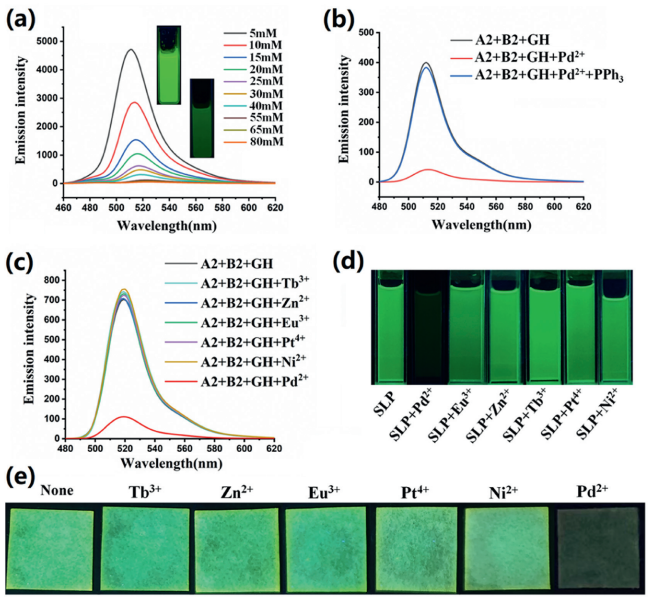

Fig. 7. (a) Fluorescence spectra of A2+B2+GH ($CHCl_3$:CH_3COCH_3 = 3:1) at different concentrations, the inset is the picture of the solution under the irradiation of 365 nm UV lamp. (b) Fluorescence emission spectra of A2+B2+GH, A2+B2+GH+$PdCl_2(PhCN)_2$, and A2+B2+GH+$PdCl_2(PhCN)_2$+PPh_3 (A2:B2:GH:Pd^{2+}:PPh_3 = 1:1:1:1:2, A2 = 0.1 mmol/L). (c) Fluorescence response of A2+B2+GH upon adding different metal ions. (d) The photoluminescence photographs of the mixtures of supramolecular polymer SLP and different metal ions. (e) Test paper strips for ion detection.

The self-repairing ability of gel was then investigated. It was observed that the visible fracture of gel automatically healed after a few minutes (Fig. 5d). This suggested that the gel possessed self-repairing ability. The reversible noncovalent interactions present in the gel network are responsible for its self-healing capability. When the sample was cut, the noncovalent bonds at the split edge were disrupted but could recover quickly due to their reversible and dynamic nature, thus initiating the healing of the gel crack. The supramolecular gel property was further investigated through rheological analysis. The gel was firstly prepared by A2+B2+GH+$PdCl_2(PhCN)_2$ (in a molar ratio of 1:1:1:1, A2 = 180 mmol/L). During the frequency sweep (Fig. 6a), it was consistently observed that the storage modulus (G') was higher than the loss modulus (G''). This suggests the presence of a supramolecular gel network formed through host-guest interactions and metal coordination [40]. The strain sweep test conducted on the gel sample revealed that G'' surpassed G' when the strain exceeded 123% (Fig. 6b). This indicates damage to the crosslinking net under large strain, where the viscous property of the sample became predominant when the network was damaged under higher strain. The step strain experiment was also performed to investigate the self-repairing behavior of gel. During the step strain sweep, the gel sample was subjected to strains ranging from 300% to 0.1% at a frequency of 10 rad/s. At high strains, damage to the gel was observed as G'' exceeded G' (Fig. 6c). However, when the strain was reduced from 300% to 0.1%, there was a rapid recovery in both G' and G'' values, indicating that the network structure of the gel could be restored quickly due to its dynamic reversibility of noncovalent interactions. This trend was consistently observed in several cyclic strain scan experiments, confirming that SCP gel possesses excellent self-repairing ability. Subsequently, the thermal stability of the gel was investigated through thermogravimetric analysis (TGA), prior to testing, the solvent was removed from the gel to form a xerogel at ambient temperature. The TGA results demonstrated minimal decomposition within the temperature range of 25–198 °C (Fig. 6d). However, a significant weight loss ranging from 3.7% to 46.1% was observed after the temperature varied from 199 °C to 441 °C. This substantial decrease in weight primarily resulted from the decomposition of crown ethers.

As the monomer A2 incorporated the Boron-dipyrromethene (BODIPY) moiety, we subsequently investigated the fluorescence characteristics of SLP constructed by A2+B2+GH. As the monomer concentration in SLP increased, the fluorescence intensity gradually weakened (Fig. 7a). The decrease in fluorescence emission was mainly caused by aggregation-induced quenching during supramolecular polymerization. Additionally, adding $PdCl_2(PhCN)_2$ to the solution of A2+B2+GH also resulted in a decrease in fluorescence emission due to the formation of a crosslinked network of SCP (Fig. 7b and Fig. S18 in Supporting information). However, when 2 equiv. PPh_3 was added to the solution of A2+B2+GH+$PdCl_2(PhCN)_2$, the fluorescence emission was restored as adding PPh_3 drove the reformation of SLP. Interestingly, no decay in fluorescence was observed when other metal ions (Zn^{2+}, Eu^{3+}, Tb^{3+}, Pt^{4+}, Ni^{2+}) were added to the solutions containing A2+B2+GH (Figs. 7c and d). Overall, the experiments have indicated that strong metal coordination between Pd^{2+} and 1,2,3-triazole moiety holds significant importance in the formation of SCP and its fluorescence emission performance. In order to further investigate the practicality of supramolecular polymers, test paper strips for ion detection were prepared (Fig. 7e). The test papers were soaked in 5 mmol/L solutions of A2+B2+GH for 10 min and then dried naturally. When different metal ions were dripped onto the test papers, only Pd^{2+} exhibited a noticeable decrease in fluorescence. These results indicate that the test paper containing supramolecular polymer shows significant selectivity towards Pd^{2+}. The successful application of supramolecular polymer enables real-time detection of Pd^{2+}.

In summary, we synthesized three distinct monomers named A2, B2, and GH. By combining these monomers at high concentrations, they underwent self-assembly to form a linear supramolecular polymer (SLP) through dual host-guest interactions. Rod-shaped fibers could be pulled from the SLP solution. Upon introducing $PdCl_2(PhCN)_2$ into the SLP solution, a structural transformation occurred as SLP converted into a supramolecular crosslinked polymer (SCP) *via* metal coordination interaction. This transition from SLP to SCP resulted in the fluorescence quenching, test paper strips for ion detection experiment confirmed that the SLP had good detection ability for Pd^{2+}. Moreover, when the concentration exceeded

145 mmol/L, the SCP further transformed into an SCP gel which exhibited various responsive behaviors such as sensitivity towards K^+ ions and temperature changes, accompanied by a reversible transition between sol and gel states. Additionally, rheological analyses confirmed that the gel possessed excellent self-healing properties.

Declaration of competing interest

The authors declare that they have no known competing financial interests or personal relationships that could have appeared to influence the work reported in this paper.

CRediT authorship contribution statement

Shengyong Liu: Writing – original draft. **Hui Li:** Writing – review & editing. **Wei Zhang:** Software. **Yan Zhang:** Methodology. **Yan Dong:** Data curation. **Wei Tian:** Writing – review & editing.

Acknowledgments

This work was supported by the National Natural Science Foundation of China (Nos. 22161020, 22022107, 21801100), the Natural Science Foundation of Jiangxi Province (No. 20212BAB203014), and the Program of Qingjiang Excellent Young Talents, Jiangxi University of Science and Technology.

Supplementary materials

Supplementary material associated with this article can be found, in the online version, at doi:10.1016/j.cclet.2024.110465.

References

[1] T. Aida, E.W. Meijer, S.L. Stupp, Science 335 (2012) 813–817.
[2] T. Hirao, H. Kudo, T. Amimoto, T. Haino, Nat. Commun. 8 (2017) 634.
[3] J. Li, J.X. Wang, B.Z. Tang, et al., Chem. Soc. Rev. 49 (2020) 1144–1172.
[4] Y.X. Liu, L.L. Wang, F.H. Huang, et al., Chem. Soc. Rev. 53 (2024) 1592–1623.
[5] H.G. Nie, X.L. Ni, Y. Liu, et al., Chem. Rev. 122 (2022) 9032–9077.
[6] T. Kakuta, T. Yamagishi, T. Ogoshi, Acc. Chem. Res. 51 (2018) 1656–1666.
[7] Y. Li, F.H. Huang, S.C. Yin, et al., Acc. Chem. Res. 57 (2024) 1174–1187.
[8] Z. Gao, Y.F. Han, F. Wang, et al., Acc. Chem. Res. 51 (2018) 2719–2729.
[9] Z.Y. Wu, H.W. Qian, L.Y. Wang, et al., Chin. Chem. Lett. 35 (2024) 108829.
[10] H.J. Wang, W.W. Xing, Y. Liu, et al., Chin. Chem. Lett. 35 (2024) 109183.
[11] I.S. Choi, N. Bowden, G.M. Whitesides, Angew. Chem. Int. Ed. 38 (1999) 3078.
[12] S. Chen, Z.K. Li, J.T. Zhu, et al., Angew. Chem. Int. Ed. 61 (2022) e202203876.
[13] L.Y. Zhao, L. Cheng, L.P. Cao, et al., Angew. Chem. Int. Ed 63 (2024) e202405150.
[14] F.Y. Cui, Q.N. Zhang, L.Y. Wang, et al., Chin. Chem. Lett. 35 (2024) 110061.
[15] K. Xu, B. Li, C.J. Li, et al., Angew. Chem. Int. Ed. 61 (2022) e202203016.
[16] C.H. Wang, Y.M. Zhang, Y. Liu, et al., Chin. Chem. Lett. 33 (2022) 2447–2450.
[17] H. Zhu, J. Liu, F.H. Huang, et al., J. Am. Chem. Soc. 145 (2023) 11130–11139.
[18] T.X. Xiao, J. Wang, L.Y. Wang, et al., Chin. Chem. Lett. 32 (2021) 1377–1380.
[19] K. Jalani, A.D. Das, S.J. George, Nat. Commun. 11 (2020) 3967.
[20] Z.Y. Li, Y.Y. Zhang, H.B. Yang, et al., J. Am. Chem. Soc. 136 (2014) 8577–8589.
[21] R.X. Bai, Z.M. Zhang, X.Z. Yan, et al., J. Am. Chem. Soc. 145 (2023) 9011–9020.
[22] Q. Zhang, D.T. Tang, S.C. Yin, et al., J. Am. Chem. Soc. 141 (2019) 17909–17917.
[23] J. Fox, J.J. Wie, S.J. Rowan, J. Am. Chem. Soc. 134 (2012) 5362–5368.
[24] H.H. Duan, T. Yang, L.P. Cao, et al., Chin. Chem. Lett. 35 (2024) 108878.
[25] Y. Zhu, H. Jiang, H.B. Yang, et al., Nat. Commun. 14 (2023) 5307.
[26] H. Peng, X. Ji, F.H. Huang, et al., Prog. Polym. Sci. 137 (2023) 101635.
[27] S. Li, K. Liu, C.J. Li, et al., Nat. Commun. 13 (2022) 2850.
[28] G.F. Li, J. Zhao, X.Z. Yan, et al., Angew. Chem. Int. Ed. 61 (2022) e202210078.
[29] H. Li, Z. Huang, W. Tian, et al., Macromolecules 57 (2024) 1328–1336.
[30] Y.F. Han, Y.K. Tian, F. Wang, et al., Chem. Soc. Rev. 47 (2018) 5165–5176.
[31] T.X. Xiao, X.X. Li, L.Y. Wang, Chin. Chem. Lett. 35 (2024) 108618.
[32] H.W. Qian, T.X. Xiao, R.B. Elmes, et al., Chin. Chem. Lett. 34 (2023) 108185.
[33] Z.Y. Wang, C. Sun, R.B. Wang, et al., Angew. Chem. Int. Ed. 134 (2022) e202206763.
[34] K. Yang, F.H. Huang, G.C. Yu, et al., Angew. Chem. Int. Ed. 61 (2022) e202213572.
[35] P. Verma1, A. Singh, T.K. Maji, et al., Nat. Commun. 12 (2021) 7313.
[36] Z.Y. Wu, H.W. Qian, L.Y. Wang, et al., Chin. Chem. Lett. 35 (2024) 108829.
[37] K.X. Teng, L.Y. Niu, Q.Z. Yang, et al., Chem. Sci. 13 (2022) 5951–5956.
[38] X.F. Ji, F.H. Huang, J.L. Sessler, et al., Chem. Soc. Rev. 48 (2019) 2682–2697.
[39] Z.Q. Wang, X. Wang, Y.W. Yang, et al., Adv. Mater. 36 (2024) 2301721.
[40] L.N. Xu, S.C. Yin, P.J. Stang, et al., J. Am. Chem. Soc. 140 (2018) 16920–16924.
[41] R.W. Tang, Y.P. Ye, Y. Yao, et al., Chin. Chem. Lett. 34 (2023) 107734.
[42] H. Li, S.H. Rao, W. Tian, et al., iScience 26 (2023) 106023.
[43] P.F. Wei, X.Z. Yan, F.H. Huang, et al., Chem. Soc. Rev. 44 (2015) 815–832.
[44] D. Zhao, Z. Zhang, X.Z. Yan, Angew. Chem. Int. Ed. 63 (2024) e202402394.
[45] Y. Zhu, W. Zheng, H.B. Yang, et al., Chem. Soc. Rev. 50 (2021) 7395–7417.
[46] C.J. Lu, S.C. Yin, P.J. Stang, et al., J. Am. Chem. Soc. 140 (2018) 7674–7680.
[47] Y.J. He, T.H. Tu, Y.T. Chan, et al., J. Am. Chem. Soc. 139 (2017) 4218–4224.
[48] T.R. Cook, Y.R. Zheng, P.J. Stang, Chem. Rev. 113 (2013) 734–777.
[49] H.B. Cheng, X.Q. Cao, J.Y. Yoon, et al., Adv. Mater. 35 (2023) 2207546.
[50] J. Wang, Q.B. Gong, E.H. Hao, et al., Coord. Chem. Rev. 496 (2023) 215367.
[51] C.J. Zhang, S.J. Li, F.H. Huang, et al., Org. Lett. 9 (2007) 5553–5556.
[52] C.J. Li, K. Han, X.S. Jia, et al., Chem. Eur. J. 19 (2013) 11892–11897.
[53] T.X. Xiao, L.Y. Wang, Y. Pan, et al., Chem. Commun. 49 (2013) 8329–8331.
[54] T. Liu, S. Wang, W. Tian, et al., Polym. Chem. 8 (2017) 1306–1314.